J. Korean Earth Sci. Soc., v. 35, no. 5, p. 313–323, September 2014
http://dx.doi.org/10.5467/JKESS.2014.35.5.313
ISSN 1225-6692 (printed edition)
ISSN 2287-4518 (electronic edition)

Spectroscopic Study of the Symbiotic Star CI Cyg

Siek Hyung*

Department of Earth Science Education (Astronomy), Chungbuk National University, Chungbuk 361-763, Korea

Abstract: We secured the high dispersion spectra of the symbiotic star CI Cyg. The HI, HeI, and HeII line profiles were analyzed using the relatively long exposure data including 1800 sec (Sep. 12, 1998, phase=0.90), 3600 sec (Aug. 12, 2002, ϕ=0.47), and 1800 sec (Oct. 21, 2009, ϕ=0.54). Although a minor outburst was reported in 2008, our three observation periods were generally known to be quiescent in earlier photometric studies. With the help of hydrodynamic simulations, we identified the two emission zones responsible for the blue- and red-shifted line components: (a) an accretion disk around a hot white dwarf star which consists of the outer cool HeI emission zone and the inner hot HeII emission part, and (b) a high density zone near the inner Lagrangian point responsible for the HeI line flux variation and the broadening of its line profile. The HeII line fluxes indicate that the HeII emission zone of the accretion disk is relatively stable, implying a constant gas inflow from the giant star throughout the quiescent period. The 2002 HeI data showed that the notable mass flow activity through the inner Lagrangian point occurred during this period and its flux intensity became strongest, whereas the HeII line width in the same period indicates that its flow activity forced the accretion disk to expand. The [OIII] lines were observed in 1998 but not detected in 2002 and 2009, implying the disappearance of the low density zone. Based on our kinematical studies upon the line profiles, we conclude that CI Cyg was stable in 1998 among the three observation periods selected in this research.

Keywords: spectroscopy, line profile, symbiotic star, CI Cyg, SPH simulation.

Introduction

A symbiotic star is a type of binary star system that consists of an evolved cold giant star, a hot star (usually a white star), and an extended ionized nebula. Hence, one can observe K or M type spectra along with the hot spectral components from a main sequence or a white dwarf star. Symbiotic stars are different from a typical star that follows the normal stellar evolution track on the H-R diagram, since they show not only absorption lines of a late type giant star but also recombination (permitted) HI, HeI, HeII and a few other forbidden emission lines.

CI Cyg (or CI Cygni) shows a long term periodic brightness change and a radial velocity variation in spectra due to the orbital motion and eclipse. A sudden brightness change caused by an outburst was reported (Aller, 1953). The UV continuum appears to be a A- or B-spectral type from a single star, but the optical and IR wavelengths cannot be explained by such spectral energy distribution of a single star. As reported from previous spectral study, e.g., AG Peg (Kim, 2004), its cool giant is large enough to fully fill up its Roche lobe (Mikolajewska and Ivison, 2001).

The earlier studies were done with UBVRI photometries (Dmitrienko, 2000) or relatively low spectral resolution observation data ($\lambda/\Delta\lambda \sim 1000$), using either ground telescopes or space telescopes (IUE and GHRS/HST, see Mikolajewska et al., 2006). It underwent a major outburst between 1970-1978 and returned to flat until a minor outburst in 2008. The high dispersion spectroscopic data ($\lambda/\Delta\lambda \sim 30000$) studies have an advantage in subtracting the detailed kinematical information from them. In this work, we analyzed the high dispersion spectral line profiles of CI Cyg observed in 3 different periods. Table 1 gives

*Corresponding author: hyung@chungbuk.ac.kr
Tel: +82-43-261-2726
Fax: +82-43-271-0526

Table 1. Basic data for CI Cyg

object	RA (h m s)	DEC (^{o} ' ")	orbital period (d)	spectral type	radial velocity (km s^{-1})
CI Cyg	19 50 07	35 41 22	855.25	A, M4	+13.86

Table 2. Observation log

Obs. date (UT)	Julian date	Phase (ϕ)	Exp. time (sec)	Wavelengths (Å)	Observatory (Detector)
1998/09/12	2451155.777	45.90	600	3450-10300	Lick (HES)
1998/09/12	2451155.751	45.90	1800	3465-10300	Lick (HES)
2002/08/12	2452498.809	47.47	300	3430-9930	Lick (HES)
2002/08/12	2452498.834	47.47	3600	3430-9930	Lick (HES)
2009/10/21	2455126.001	50.54	1800	3520-9230	BOAO (BOES)

Lick observatory is at Mt. Hamilton in US, BOAO is at Bohyunsan in Korea.

the basic data for CI Cyg.

Section 2 describes the observation and theoretical simulation. Section 3 presents the analysis of the line profiles of H and He lines. Conclusions are given in Section 4.

Observation Phases and SPH Simulation

The spectroscopic observations had been carried out on 1998 September 12 and 2002 August 12 (UT) using the Hamilton Echelle Spectrograph (HES) attached to the 3-m Shane Telescope at Lick Observatory, and on 2009 October 21 (UT) using the Bohyunsan Optical Echelle Spectrograph (BOES) attached to the 1.8-m telescope at Bohyunsan Optical Astronomy Observatory (BOAO). The weather condition was very clear through the nights in 1998 and 2002. The seeings were ~1.5" and 1.0" in 1998 and 2002, respectively, but ~3" in 2009 due to bad weather. The slit widths were set to 1.2" in 1998 and 2002 (HES), but the BOES fiber diameter was 3" in 1998. For the flux and blaze function corrections, we observed the standard star 58 Aql. The former 2 series observations were done by Hyung and Aller, while the latter observation was done by Hyung and Dr. Lee. Table 2 shows the observation log. Successive columns are observation date (UT), its corresponding Julian day (JD), the orbital phase (ϕ), exposure time, coverage wavelength range by the spectrograph, and observatory. The orbital phase (ϕ) has been calculated based on the following equation (Aller, 1953),

JD (min)=JD (2411902)+855.25*E

where JD (min) is the reference ephemeris for the primary minima and E is a number of an orbital period, P=855.25 days after the first defined photometric minimum epoch. The 1998 data correspond to E=45 (ϕ=45.90).

Fig. 1 shows schematically a white dwarf (WD) and a giant star (GS) in CI Cyg at 3 phases, ϕ=0.90, 0.47, and 0.54 for 1998, 2002, and 2009, respectively. The arrow ($\rightarrow$) represents the line of sight. We assume inclination angle i=90^o in this diagram. Iijima (1982) deduce the WD and GS masses are 0.6-0.7 and 2.4 $M_\odot$. We assume that the WD to GS mass ratio is 1:3 and the relative radii of two stars from the center of mass (CM) are 3:1. Two stars are assumed to revolve each other counter-clockwise direction. The physical parameter of the compact hot star in CI Cyg is still controversial. Kenyon et al. (1991) argued that the hot source should be a 0.5 $M_\odot$ main-sequence star, surrounded by an extended disc, at an accretion ratio of M~1-3×10^{-5} $M_\odot$ yr^{-1}. Since both stars are assumed to be revolving counter-clockwise, the outflow gas shell around the GS and the inflow gas around the WD must rotate in the same counter-clockwise direction.

Some fraction of the outflowing gas from the GS may be transferred to the WD through the inner Lagrangian point L_1 with the amount dependent on the GS radius and the physical condition. Note that the

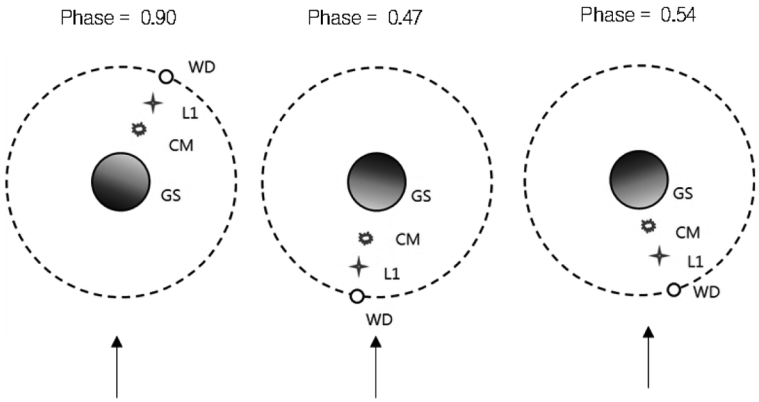

Fig. 1. The schematic diagram showing the orbital motion of the two components in CI Cyg. The left, middle, and right one show the position of components in 1998, 2002, and 2009. ✲ means CM (center of mass). GS means giant star. WD means white dwarf. † means Lagrangian point, L_1.

orbital movement directions of two stars are very close to the tangential direction in the case of our observing epochs, i.e., perpendicular to the line of sight. Hence, the gas shells around the two stars must move to the tangential directions, i.e., V=0 km s^{-1} (if they move along the same direction as the stars do and as long as they are not gravitationally bound to the stars). However, the escaping gas from the GS expands radially outward in all directions.

CI Cyg and all other symbiotic stars are nearly a point object in observation and there is no way of figuring out the proper physical parameter accurately. To help our understanding, we tried a preliminary simulation for CI Cyg with a smoothed particle hydrodynamics (SPH) method (Lucy, 1977). Details were described elsewhere, e.g., Mastrodemos and Morris (1998). Our preliminary simulation runs do not match the observed values suggested by some of earlier studies, e.g., Iijima (1982): stellar masses and the separation between them, are not refined. The mass rato of the two stars was assumed to be 1/3, i.e., WD:GS=1:3 (e.g., 0.5 $M_\odot$:1.5 $M_\odot$), with the mass loss rate of the GS, 6.5×10^{-5} $M_\odot$ yr^{-1}. If one devises the calculation with a smaller time step size or the large number of particles, one must suffer the computer time increase to see the result. In the simulations, we set each calculation time step to be (Δt)=0.4 day. We performed various simulations until the final time step reached t~10-15 yrs in real time scale.

In Fig. 2, we present one snap shot of simulations, that might be CI Cyg at ϕ~0.8, similar to the one in Fig. 1a. Fig. 2a shows the face-on view, similar to Fig. 1a, while Fig. 2b shows an edge-on view. The arrows in Fig. 2a show the velocity vectors of the gas outflows from the GS. The final number of SPH particles is about 40000 and the result was at a time step, t~12 yrs. Although the simulation result does not exactly represent the actual physical parameter of CI Cyg, it has a number of useful suggestions on the inflow gas distribution around the WD and the outflow activity from the GS.

The hot WD UV photons cannot reach the outer part of the outflowing gas shell and they cannot ionize all of the expelled gas from the GS (Fig. 2). The ionized part would be a small zone, close to the WD. Hence, we must pay attention to the geometry of the WD and its surrounding to interpret the spectral line profiles. We know that the WD has an accretion disk formed with outflowing gas from the GS component. The expanding gas from the GS must pass the inner Lagrangian point to reach the WD (assuming that the Roche lobe was not filled). Since the GS is believed to be large enough to obstruct the bright emission zone around the WD, the front expanding gas of the GS may obstruct the front approaching side (as blue component in line profile) than the receding rear side.

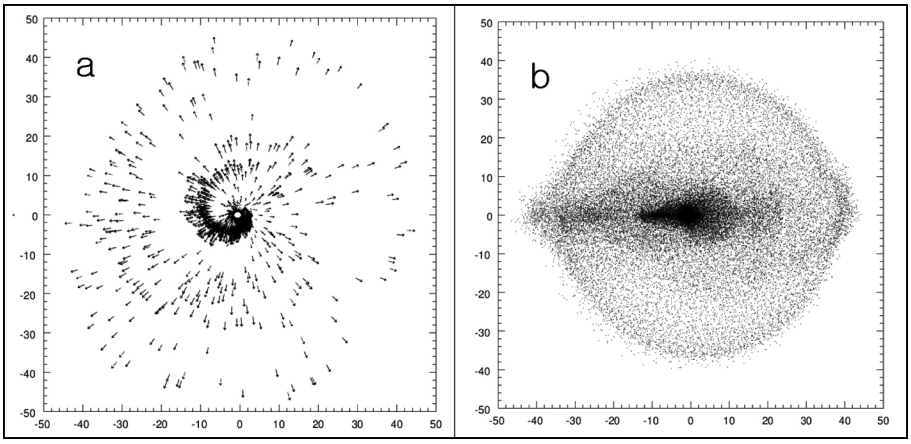

Fig. 2. A simulation diagram showing the orbital motion of two components in CI Cyg and gas outflow from a GS. Some fraction of the GS outflow transfer into a WD after passing an inner Lagrangian point. (a) The face-on view. The GS is a circle at the center and the observer (the line of sight) is at bottom of the box. The WD (not clearly seen, here) is at position angle, PA~ –40°. (b) The edge-on view. Due to a thick gas, both stars cannot be seen but the observer above the figure. X and Y axis units: AU.

In such a case, the spectra might have a blue component of higher intensity. In the case of a small radius GS, the WD will be a key factor in understanding the emission component.

Our observation periods were not exactly an eclipsing moment as seen Fig. 1a. The approaching gas zone in Fig. 2a or Fig. 1a would become the receding gas in half period later (as in Fig. 1b and Fig. 1c. In the following section, we present the strategically important line profiles with regard to the relative positions of two stellar components in each orbital phase.

H and He lines

The temperature and the spectral type of both stars may change. We employed the M3, M4, M5 standard stars for GS component, HD40472, HD44272, and HD56889, to discern the WD lines and their variation of line intensities in CI Cyg. The UV photons that excite the gas are known to come from the pseudo-photosphere of the WD. Since we do not quantitatively analyze the flux intensities of emission lines, we will not bother the spectral energy distribution of the pseudo-photosphere or the WD. We will limit our study to the line profile components and their variation during our three observing periods. Line profiles were analyzed using the echelle spectra reduction package in IRAF (image reduction and analysis facility) software written at the National Optical Astronomy Observatory (NOAO) and ESO StarLink/Dipso reduction package. With the IRAF, we obtained the wavelength and flux calibrated data, and finally we had the final spectral data in the optical wavelengths. Then, we examined all the data to see if there are any useful emission or absorption lines to extract kinematical information for all the 10, 30 min (1998, Sep. 12), 5, 60 min (2002, Aug. 12), and 30 min (2009, Oct. 21) spectra, respectively. For our study, we used only the longer exposures of 30 min and one 60 min.

Finally, we transformed the horizontal axis of the spectra from the wavelength to the velocity scale in IDL package. All the available line profiles have been compared one another to see whether they are real. The strength and width of each component were all reviewed in the same velocity frame, ΔV=200 km s^{-1}, e.g., from –100 km s^{-1} to +100 km s^{-1}. There might be a small error in the radial velocity information introduced by the wavelength calibration, but it would not change our conclusion. Since the is very broad, we examined this line profile more carefully, in a broader lower and upper limit, e.g., –300 km s^{-1} and +300 km s^{-1}. With the Dipso, we decomposed each

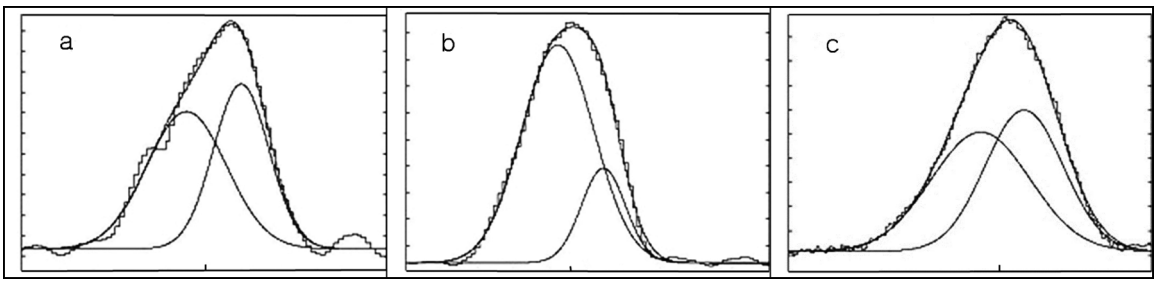

Fig. 3. HeI 7065 line profiles in three periods. (a) 1998 (30 min): we define the blue on as 'I' and the red one as 'II'. (b) 2002 (60 min). (c) 2009 (30 min). The horizontal velocity widths (band-paths) are ΔV=200 km s^{-1} and the tick mark at the center is V=0 km s^{-1}. The vertical flux unit is erg cm^{-2} $Å^{-1}$ s^{-1}. The absolute flux values are not specified. See Table 3.

line profile into two or three components and later we further investigated as to how these components get involved with the structure of CI Cyg.

Fig. 3 shows the decomposed line profiles of HeI 7065 observed in three observing runs. The flux scales (erg cm^{-2} $Å^{-1}$ s^{-1}) are not given (the specific flux values are important in this study). The HeI lines as well as the HI ones are also observed in all of three periods. The reason why we chose the HeI line instead of HI lines is that the HI lines represent the mixed whole nebula zone. All the HeI line profiles consist of two Gaussian components, implying there are two major emission zones in CI Cyg.

In any single object double Gaussian components are not special as long as the two component shapes are about the same. A symmetrical or closely similar double Gaussian line profiles can be formed in any spherically symmetrical shell object, such as spherically symmetrical or ring type planetary nebulae due to the stratification effect (Lee and Hyung, 2007; Lee and Hyung, 2008). Since there is an accretion disk around the WD in CI Cyg, the rotating nebulous disk may form roughly symmetrical double component profiles. However, the observed HeI line profiles imply that the emissions are not from such a simple symmetrical structure or an ellipsoidal sphere. One cannot completely ignore a presence of the symmetrical accretion disk structure around the WD. Admitting the accretion disk structure in CI Cyg, we look of another structure such as the outflow gas activity from the GS and its inflowing path to the WD.

Fig. 3 shows that the line consists of a broader blue component and a sharper blue component. Note that not only the flux intensity but also the width of each line component varied. The narrowness or sharpness implies the coherent emission zone, while the broad line width suggests a complex emission region. The broader or narrower shape of the line profiles also involve the gas flow activities. The profile shape also involves the orbital motions of the system: whether the emission becomes a red or a blue component is determined by the location of the emission zone: the left- or the right-side relative to the CM. It may also depend on the physical condition of both stars. From Fig. 3a, we define the broader blue-shifted one as 'I' and the sharper red-shifted one as 'II'.

Assuming that the gas expands radially outward from the GS and also assuming that most emission comes from the zone close to the WD, Fig. 1 implies that there will be a positional change of the WD from 1998 to 2009. Fig. 2 indicates most gas around the WD will flow away along the line (that is farther away from the GS). The emission zone around the WD changes its position from the rear side of the GS (or farther away from us than the GS or CM) to the front one (close to us). The relative position of the inner Lagrangian point L_1 also changes. Although the arrow marks in Fig. 2 seem to indicate that most gas around the WD (as in Fig. 1a) recedes from us, there will be a large fraction approaching due to the accretion disk rotation (Appendix Fig. A).

Considering the orbital motion and accretion

activity, the blue-shifted component (I) in Fig. 3a, responsible for the approaching zone in Fig 1, will become the red-shifted component in Fig. 3b responsible for the receding zone in Fig. 1. In a similar way, the receding zone in Fig. 1, responsible for the narrow red component (II), in Fig. 3a, will become a blue component in Fig. 3b, due to its relative positional change to the observer as seen in Fig. 1. Nonetheless it is about the same in its characteristics between the 2002~Fig. 3b and the 2009~Fig. 3c unless there is any change in stellar activities. Hence, the zone responsible for the red line component (I) in Fig. 3b must correspond to the same zone responsible for the same red one in Fig. 3c. Moreover, the blue component (I) in Fig. 3a must correspond to the red in Fig. 3b and Fig. 3c. Note that (1) the predefined 'I' component changes its Doppler shift position: blue→red→red from Fig. 3a to Fig. 3b to Fig. 3c; and 2 the other 'II' component accordingly does so: red→blue→blue from Fig. 3a to Fig. 3b to Fig. 3c.

In Table 3, we list the measured line fluxes (erg cm^{-2} $Å^{-1}$ s^{-1}) and FWHM (in km s^{-1}) of HeI 7065 for all three observations, and we illustrate the same data in Fig. 4. Although the observing periods were known to be quiescent, there were a notable change in both flux intensities and full width at half maximum (FWHM) of HeI line profile components.

The fluxes are given in erg cm^{-2} $Å^{-1}$ s^{-1}; FWHM (full width at half maximum) in km s^{-1}. X (–Y) means $X\times10^{-Y}$. The boldface numbers are for the component I, and the rest figures are for the component II (see the text).

Note that both HeI line flux components increased in 2002. Especially, the component II flux exceeded the 1998 by 7 times. The component II which was narrower in 1998, became dispersed in 2002, i.e., the FWHM is broader than the I component (46.7 vs. 28.4 km s^{-1}). The increased FWHM indicates that the II emission zone became complicated, or the emission zone expanded into a kinematically complicated region. The flux intensities of both HeI components became weaker in 2009, but the FWHM of the II component became even more broader. Since the HeI lines form

Table 3. HeI 7065 flux and FWHM measurement

year		1998	2002	2009
line flux	blue	**3.64(-11)**	2.03(-10)	7.23(-12)
	(err)	**±7.03(-12)**	±1.03(-11)	±8.17(-13)
	red	3.03(-11)	**5.36(-11)**	**5.40(-12)**
	(err)	±7.00(-12)	**±9.73(-12)**	**±8.26(-13)**
FWHM	blue	**51.0**	46.7	59.9
	(err)	**±4.4**	±1.20	±2.21
	red	35.5	**28.4**	**47.4**
	(err)	±2.20	**±1.55**	**±1.31**

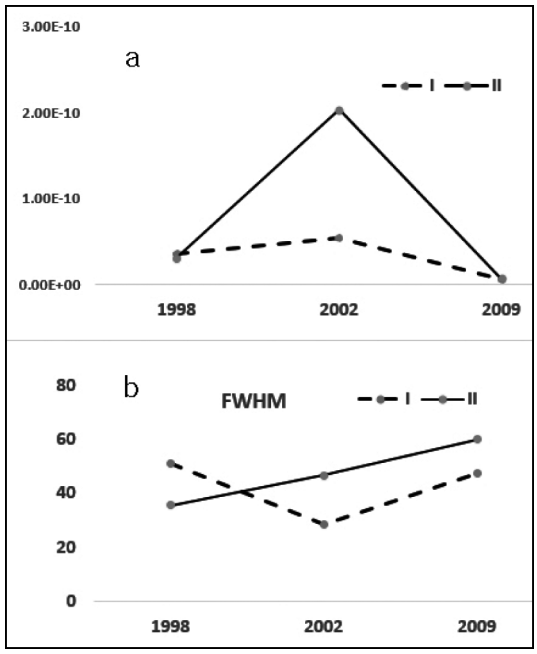

Fig. 4. HeI 7065 fluxes and FWHMs of observing 3 periods. (a) flux intensity in erg cm^{-2} $Å^{-1}$ s^{-1}. (b) FWHM in km s^{-1}. Dashed line: I. Solid line: II. See Table 3.

in the relatively low excitation line, it implies the physical condition of the distant zone (outer part shell) from the WD. The major emission source responsible for both I and II components (both blue- and red-shifted components) might be the outer (so relatively cool) zone of the accretion disk around the WD, The additional heating might be added to the II component and as a result the line profiles become stronger and broader in 2002 (and perhaps 2009 as well). The additional heating source is probably the emission from the flowing zone located somewhere between two stars.

Table 3 and Fig. 4 indicate that the mass-flowing from the GS and the accretion into the WD were most active in 2002 among our observing periods. The mass transfer activity (or inflow gas amount) around the inner Lagrangian point and its resulting formation of an accretion disk (shell) around the WD, must be changed radically during this period. However, we believe that there was no significant change in geometry (relative position) and physical conditions of both stars, GS (donator) and WD (receiver). between 2002 and 2009 (in Fig. 2). The difference of line profiles between 2002 and 2009 must be caused by the slight change of the gas flow activity from the GS and a change in gas viscosity of the inner Lagrangian point, L_1, (i.e., approaching and receding zones in CI Cyg). The density of this inner Lagrangian zone might become temporarily increased, due to the increased gas flow near the L_1 point. The additional contribution to the broadening of the II component in 2002 (blue one) is likely due to the change of gas outflow from the RG surface that passes through L_1 that heated by the hot WD photons.

Knowing the accretion process accurately is not a simple matter. Depending on the physical parameters of the gas shell and WD, a large portion of the expelled gas from the GS might escape into space in a hyperbolic path without reaching WD or it might form a shallow accretion disk (Appendix Fig. Aa and Ab). The inner Lagrangian point is the most likely place where a high density gas is found. The high density gas at this point is close enough to face the hardened UV photons from the WD or its hot accretion disk. The high viscosity of the high density inner Lagrangian point might also change the flowing gas speed and its related geometry. As a result, some fraction of the expelled gas from the GS might arrive at the WD surface and heating WD to a high temperature (but not quite enough for a huge explosion at the surface: see Fig. Ac in Appendix). The detailed treatment is beyond the scope of the present study. One must carefully investigate the hydrodynamic and nuclear burning activity of the flow in a future gas dynamic study.

The high excitation HeII lines were also observed in all of three observing runs, suggesting that there had been enough (nearly constant) gas inflow to an accretion disk shell. Fig. 5 shows the HeII 5412 and HeII 4686 line profiles. They have a single Gaussian component, implying that the geometrical structure of the emission zone is fairly symmetrical. Its involving accretion disk is either ellipsoidal or a torus type. Since the high excitation HeII lines ought to be formed in a high gas temperature zone, one can guess that the HeII emission is mainly from an accretion disk related structure close to the WD. The SPH simulation in Fig. 2 or Appendix Ac diagram indicates that the active accretion activity can create a spiral - axially non-symmetrical - structure around a WD. However, the HeII line profiles of the three observation periods show a single Gaussian profile, indicating that the structure responsible for the HeII lines is symmetrical, i.e., a stable accretion disk structure of circular rotation. The spiral motion should be refined by the internal gas viscosity in an actual simulation.

The HeII 4686 lines were observed in all the 3 periods, but the HeII 5412 was observed only in 1998. We present the flux and FWHM measurements of HeII 4686 in Table 4. The HeII FWHMs are broader than the HeI components for the relatively quiet periods, 1998 and 2009, whereas during the active 2002, the HeII line shows a smaller FWHM. The broad line width in 1998 and 2008 implies a faster rotation of the hot accretion disk than that of the inner disk part, responsible for the HeII lines. The conditions for stable H-burning and smallest envelope radius (e.g., high temperature of the pseudo-photosphere) require a stable mass accretion rate (Kenyon, 1986 and references therein). The relatively stable accretion activity might occur in 1998 and 2009.

The most plausible explanation for the narrowness of the 2002 HeII lines is that some unstable accretion activity pushed away the inner radius, responsible for the HeII emission zone (but still smaller than the HeI disk). The large value of the radius in 2002 means a slowly rotating disk around the WD and as a result the narrower HeII line profile might be formed in

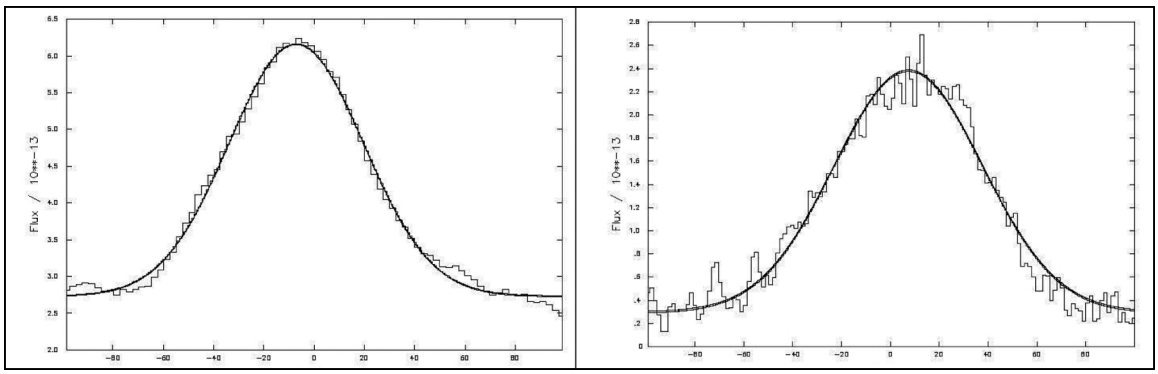

Fig. 5. HeII 5412 (Lick HES; 1998, 30 min) and HeII 4686 (BOAO BOES; 2008, 30 min).

Table 4. HeII 4686 flux and FWHM measurement

year		1998	2002	2009
line flux	blue	2.60(-10)	2.61(-10)	1.55(-11)
	(±error)	±1.07(-12)	±2.46(-12)	±2.37(-13)
FWHM	blue	64.3	42.0	70.3
	(±error)	±0.23	±0.43	±1.11

2002 than the other two periods. Any increase of the accretion rate above the amount required to sustain stable nuclear burning would cause the burning envelope to expand. If this occurs, the pseudo-photosphere would shift its energy peak from far-UV into the optical range, causing the star to appear in outburst (Siviero et al., 2009). However, the increase of the accretion rate in 2002 is not quite enough for such an outburst activity.

See Table 3 for flux unit.

Fig. 6 shows the line profiles of Hα and Hβ. Note that the line width is much broader than the Hβ or other He lines. For Hα, we set the much wider horizontal scale, –300 km s^{-1} to +300 km s^{-1} and find out three components with Starlink/Dipso software. The third broader component at the bottom does not belong to either I (blue in 1998) or II (red in 1998) component. Could this broader FWHM component indicate the third zone of much higher velocity flow? The FWHM broadening of line, i.e., 3~5 times faster than the expected gas movement, was known to be caused by Raman scattering mechanism in a place close to a high density neutral gas of column density ~10^{19} cm^{-2} near the HII zone (Lee and Hyung, 2000; Lee et al., 2012). The broader line profile component obviously does not indicate a swiftly flowing gas activity. The broadening must be due to the Raman scattering mechanism in an extremely high density zone, near the L_1 point. The relatively large amount of Lyman quanta must be present in the high density zone. Whereas, the Hß line profile and other HI line profiles (not presented here) that display a simplistic form of a double Gaussian profile as in Fig. 6b, indicate that they are not affected by such scattering.

In summary, the main structure responsible for the HI, HeI, and HeII lines is likely to be the accretion disk around the WD and the high density zone near inner Lagrangian point. The two zones must be heated by the UV photons and become fully or partially ionized. The gas flow activity near the inner Lagrangian point perhaps disturbs the density structure and as a result, CI Cyg forms different HeI and line profiles in each epochs. The effect of the latter high density zone might appear in other low excitation lines, which were not analyzed in the present study. Meanwhile, the high excitation HeII lines showing a single Gaussian component, were about the same in all the observations, indicating the stable inflow activity onto the inner accretion disk part, perhaps due to the refinement of the accretion activity by viscosity.

Conclusions

The high dispersion spectra ($\lambda/\Delta\lambda$~30000) of the symbiotic star CI Cyg were secured by the Lick

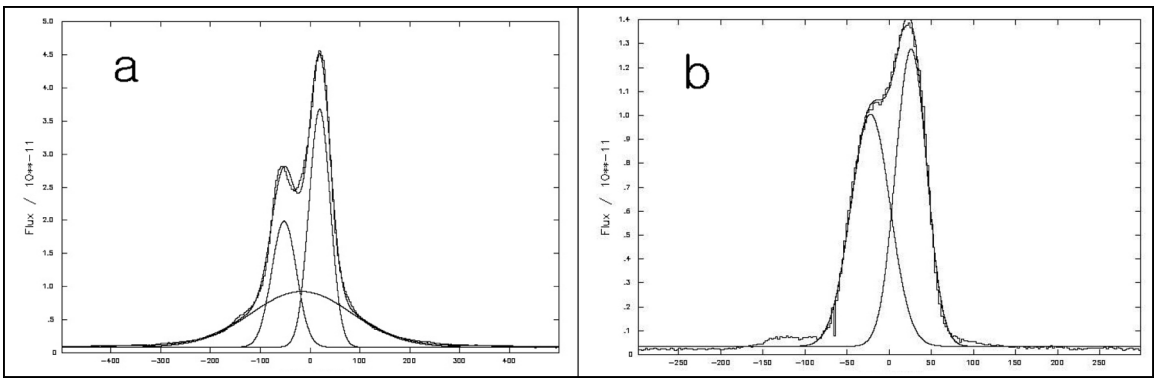

Fig. 6. Hα and Hβ line profiles (1998, 10 min). The wavelength width for (a) the Hα is broader than that for (b) the Hβ. See the text.

observatory HES and the BOAO BOES. Our three observations were done in during quiescent periods. We analyze the line profiles for three epochs to find out the origin of the flux and FWHM change of the line profiles.

We investigated the line profiles of three observing periods and tried to understand them in regard to the orbital motion of a symbiotic binary system and the mass flow activity near the inner Lagrangian point with the help of preliminary SPH simulation. CI Cyg is known to have experienced only a few outbursts in its long recorded history. i.e., minor in 1911 and 1937, a major outburst between 1970 and 1978, and a most recent minor outburst in 2008 August (Siviero et al., 2009). We found a somewhat stronger activity in 2002 spectral data,. The last 2008 activity does not seem to continue until our 2009 observing period. In 1998, the WD of CI Cyg was about to enter the eclipse, but the spectral intensities that are about the same as the 2009 spectra, shows no evidence of eclipse in 1998. The physical scale of the GS and its surrounding gas shell must be not large enough to block the emission from the accretion disk during these periods.

The FWHM or intensity of each component changed. Based on the orbital phase change, we define two components, I and II from the three differently observed HeI line profiles. We conclude that the HeI and HI lines are formed mainly in the outer part of the accretion disk and an additional zone near the inner Lagrangian point. The 'I' emission zone is most likely to be an outer part of the accretion disk. The 'II' component that appears to be formed from both the accretion disk and the inflow high density zone near the L_1 shows a large variation, indicating the complexity of the HeI emission zone responsible for it (Appendix Fig. Ac).

The HeII 5412 and HeII 4686 line profiles show a single Gaussian component, implying a perfectly symmetrical emission zone (Fig. 5). Since the high excitation HeII lines are supposed to be formed in a high gas temperature zone, we conclude that the HeII emission represents the inner part of the accretion disk. The HeII lines indicate that the physical condition or the radius of the inner accretion disk part changes.

One cannot resolve the spatial component of the symbiotic star even with a high spatial resolution space telescope, e.g., HST, since most of the gas around both stars in a symbiotic binary system is out of reach from the WD UV photons. Although one would not be able to see a shaping history of CI Cyg even with any statistical studies, the simulation study as given in Fig. 2 shows an interesting feature on gas distribution in a symbiotic system, (1) The WD UV photons cannot ionize all the outflowing gas around the symbiotic system but only a small fraction, close to the WD, seems be ionized (Fig. 2b). (2) The actual emission zone could be more concentrated on right side near the WD, as shown in Fig. 2a. Perhaps, this is the case of 2002 and 2009 spectral emissions. (3)

Fig. 2 also suggests that the cool gas in the front zone of the GS might absorb the ionized emission coming from the symbiotic star system. We do not investigate the absorption line in this study.

The two forbidden lines, [OIII] and [OI], were weakly registered in 1998 spectra. These lines are usually observed in a planetary nebula of relatively low density $<10^6$ cm^{-3}. but they were not detected in 2002 and 2009. In planetary nebulae, the [OIII] 4959 and [OIII] 5009 lines are usually stronger than the Hß line by about 10 times. The gas temperature of the HeI emission zone in CI Cyg could be very similar to that of planetary nebular gas shell. These lines represent the medium and low excitation lines like the HeI emission zone. The absence of these lines and other forbidden lines in 2002 and 2009 implies that the density of the medium and low excitation emission zone during these periods was extremely higher in the medium excitation zone. The present study does not extend to the quantitative details of the flux intensities and elemental abundances in CI Cyg. We leave this matter to the future study.

Acknowledgment

This work was supported by the research grant of Chungbuk National University in 2012. The author is grateful to the late Prof. Lawrence H. Aller of UCLA, who carried out the Hamilton Echelle observation program together with him. He also thanks for Dr. Lee, S.-J. and Ms. Lee, S.-A. who gave helps with the data reduction.

References

Aller, L.H., 1953, Spectrographic studies of the combination variables Z Andromedae, BF Cygni, CI Cygni. Publications of the Dominion Astrophysical Observatory Victoria, 9, 321-362.

Dmitrienko, E.S., 2000, UBVRI photometry of the eclipsing symbiotic system CI Cygni in 1996-1999. Astronomy Letters, 26, 520-528.

Iijima, T., 1982, CI Cyg - the stage of case C mass transfer. Astronomy and Astrophysics, 116, 210-216.

Kenyon, S.J., 1986, The symbiotic stars. Cambridge University Press, New York, USA, 295 p.

Kenyon, S.J., Oliversen, N.A., Mikolajewska, J., Mikolajewski, M., Stencel, R.E., Garcia, M.R., and Anderson, C.M., 1991, On the nature of the symbiotic binary CI Cygni. Astronomical Journal, 101, 637-654.

Kim, H., 2004, The investigation of the emission and absorption line of the high dispersion spectra of the symbiotic star AG Peg. Unpublished Ph.D. dissertation, Korea National University of Education, Chungbuk, Korea, 176 p. (in Korean)

Lee, H. and Hyung, S., 2000, Broad Ha wing formation in the planetary nebula IC 4997. The Astrophysical Journal, 530, L49-L52.

Lee, S.-J. and Hyung, S., 2008, Photoionization models for planetary nebulae. Journal of the Korean Earth Science Society, 29, 419-427.

Lee, S.-J., Hyung, S., and Lee, K.W., 2012, An analysis of the symbiotic star Z And line profile. Journal of the Korean Earth Science Society, 33, 608-617. (in Korean)

Lee, S.-M. and Hyung, S., 2007, Kinematics and geometrical structure of the planetary nebula NGC 6881. Journal of the Korean Earth Science Society, 28, 847-856. (in Korean)

Lucy, L.B., 1977, A numerical approach to the testing of the fission hypothesis. Astronomical Journal, 82, 1013-1024.

Mastrodemos, N. and Morris, M., 1998, Bipolar preplanetary nebulae: Hydrodynamics of dusty winds in binary systems. I. formation of accretion disks. The Astrophysical Journal, 497, 303-329.

Mikolajewska, J. and Ivison, R.J., 2001, On the radio spectrum of CI Cygni. Monthly Notices of the Royal Astronomical Society, 324, 1023-1028.

Mikolajewska, J., Friedjung, M., and Quiroga, C., 2006, Line formation regions of the UV spectrum of CI Cygni. Astronomy and Astrophysics, 460, 191-197.

Siviero, A., Munari, U., Dallaporta, S., Valisa, P., Luppi, V., Moretti, S., Tomaselli, S., Bacci, S., Ballardini, F., Cherini, G., Graziani, M., Frigo, A., and Vagnozzi, A., 2009, The ongoing 2008-09 outburst of CI Cyg. Monthly Notices of the Royal Astronomical Society, 3990, 2139-2145.

Manuscript received: June 23, 2014
Revised manuscript received: July 25, 2014
Manuscript accepted: August 11, 2014

Appendix

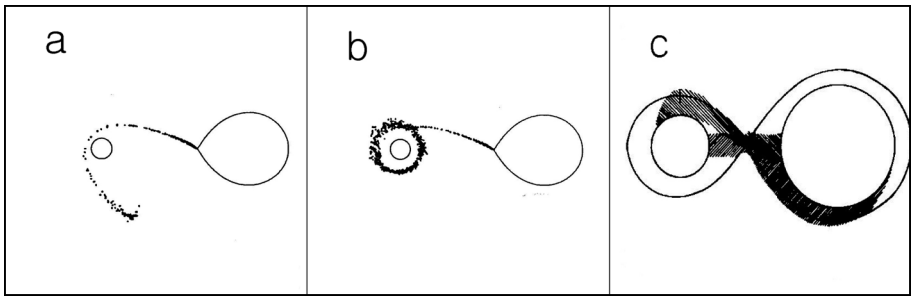

Fig. A. A schematic diagram showing 3 different cases of mass flow around a WD. GS: Small circle at the left side. In general, the flowing gas is not gravitationally bound to a GS or a WD. The actual gas flow trajectory must be calculated on a case-by-case basis using the SPH simulation. The escaping gas from the GS could either (a) pass WD and escape from it, or (b) form an accretion disc around a WD, or (c) (some fraction) land onto a WD surface. The ellipsoidal double lobe sphere in (c) represents the Roch lobe. In this diagram, the system's orbital and stellar rotation directions are assumed to be counter-clockwise.